Eur. Phys. J. C 10, 681–687 (1999)
Digital Object Identifier (DOI) 10.1007/s100529900172

THE EUROPEAN PHYSICAL JOURNAL C

Radiative effects in the processes of hadron electroproduction

I. Akushevich, N. Shumeiko, A. Soroko

National Center of Particle and High Energy Physics, 220040 Minsk, Belarus

Received: 17 March 1999 / Revised version: 18 June 1999 / Published online: 28 September 1999

Abstract. An approach to calculate radiative corrections to the unpolarized cross section of semi-inclusive electroproduction is developed. Explicit formulae for the lowest order QED radiative correction are presented. A detailed numerical analysis is performed with the kinematics of experiments with fixed targets.

1 Introduction

Semi-inclusive processes of hadron electroproduction have been recognized long ago [1] as an important tool for testing QCD predictions of the nucleon structure because them allow one to get information about the quark distributions in the nucleon for each flavour separately. A precise analysis of the hadron structure functions extracted from the experimental data requires, however, an iterative procedure involving the radiative correction (RC) of these data. Firstly, radiative effects in coincidence experiments were discussed in [2]. Covariant formulae for the RC to the cross section of semi-inclusive processes can be obtained on the basis of the Bardin and Shumeiko approach offered in [3] originally for elastic scattering. In [4] the method was developed on semi-inclusive processes, where analytical formulae for the lowest order RC for coincident processes in electroproduction were found. In this paper we present analogous formulae, but contrary to results of [4] we do not assume integration over the hadronic kinematical variables p_{t}^2 and ϕ^h. This allows one to calculate the model-independent RC relying only on the common representation for the hadronic tensor. We should point out that there are other possible frameworks to calculate the semi-inclusive RC. One of them is based on the Monte Carlo approach; e.g., at HERA the generator HERACLES [5] is used.

In recent years the cross sections of the hadron electroproduction on fixed targets were measured as functions of azimuthal angles and transversal momentum of the registered particles (see [6,7] and references therein). However, this information is not sufficient to extract all structure functions involved in the hadronic tensor in the wide kinematical region required for the RC calculation. Therefore, we have to use some model for the semi-inclusive structure functions. Such a model should give a good initial approximation for the iterative procedure, and we hope that the model for the structure functions which can be constructed on the basis of results of Mulders and Tangerman [8] is an appropriate one. It should be noted that unpolarized structure functions were considered in [8] along with the spin dependent distributions. However, in this paper we restrict ourselves only to the calculation of the RC to the unpolarized cross section. The consideration of RCs to observable quantities in polarization experiments on hadron electroproduction will be the subject of a separate publication. Notice that for azimuthal effects we additionally use a model given in [9] (see also [10]).

Thus we calculate QED radiative corrections to hadron electroproduction, which give a main contribution to the total correction in the experiments at fixed target. The pure weak corrections as well as hadronic radiation require additional assumptions about the hadronic interactions, so they are not considered here. In order to take into account the multiple soft photon radiation, the infrared corrections have to be exponentiated according to one of the several possible approaches [11]. We choose to follow the prescription of [12].

In Sect. 2 we briefly describe the kinematics of the hadron electroproduction process with and without radiation of an additional photon. The hadronic tensor and the model for the structure functions are discussed in Sect. 3. The analytical formulae for the Born cross section and for the RC of the lowest order are given in Sects. 3 and 4. In this paper, only one ultrarelativistic approximation is made: the electron mass is considered to be small. We note that the final analytical formulae are written in the form similar to that used in the FORTRAN code POLRAD 2.0 [13]. Section 5 is devoted to a numerical analysis, performed on the basis of the new code HAPRAD specially developed by us for this purpose. Most cumbersome formulae are gathered in the Appendix.

2 The kinematics

The cross section of hadron h electroproduction

$$e(k_1) + N(p) \longrightarrow e'(k_2) + h(p_h) + X(p_x) \qquad (1)$$

depends on five kinematical variables which can be chosen as

$$x,\ y;\ z,\ t,\ \phi_h, \qquad (2)$$

where x and y are the usual scaling variables, z and t are defined via the hadron momentum,

$$t=(q-p_h)^2,\quad z=p_hp/pq,\quad q=k_1-k_2, \tag{3}$$

ϕ_h is an angle between the planes $(\mathbf{k}_1,\mathbf{k}_2)$ and $(\mathbf{q},\mathbf{p}_h)$ in the rest frame ($p=(M,\mathbf{0})$). Also the following invariants will be used:

$$\begin{aligned}&S=2k_1p,\ X=2k_2p=(1-y)S,\ Q^2=-q^2=xyS,\\&W^2=S_x-Q^2+M^2,\ S_x=S-X,\ S_p=S+X,\\&\lambda_Q=S_x^2+4M^2Q^2,\\&M_x^2=p_x^2=(1-z)S_x+M^2+t,\ V_{1,2}=2k_{1,2}p_h.\end{aligned} \tag{4}$$

When the radiative process

$$e(k_1)+N(p)\longrightarrow e'(k_2)+\gamma(k)+h(p_h)+X(\tilde{p}_x) \tag{5}$$

is considered, three additional independent variables have to be introduced:

$$R=2kp,\quad \tau=qk/kp,\quad \phi_k, \tag{6}$$

where ϕ_k is the rest frame angle between the planes $(\mathbf{k}_1,\mathbf{k}_2)$ and $(\mathbf{q},\mathbf{k})$. Also we introduce the quantity $\mu=kp_h/kp$ and the following invariants:

$$\begin{aligned}\tilde{Q}^2&=(q-k)^2=Q^2+R\tau,\\\tilde{W}^2&=(p+q-k)^2=W^2-R(1+\tau),\\\tilde{t}&=(q-k-p_h)^2=t+R(\tau-\mu),\\\tilde{M}_x^2&=\tilde{p}_x^2=M_x^2+R(1+\tau-\mu).\end{aligned} \tag{7}$$

The phase space of the three final particles is parameterized as

$$\frac{\mathrm{d}^3\mathbf{k}_2}{k_{20}}\frac{\mathrm{d}^3\mathbf{p}_h}{p_{h0}}\frac{\mathrm{d}^3\mathbf{k}}{\mathrm{k}_0}=\pi S_x dxdy\,\frac{S_x\mathrm{d}z\mathrm{d}t\mathrm{d}\phi_h}{2\sqrt{\lambda_Q}}\,\frac{R\mathrm{d}R\mathrm{d}\tau\mathrm{d}\phi_k}{\sqrt{\lambda_Q}}. \tag{8}$$

Instead of the t-dependence we will also consider the cross section as a function of the transversal momentum p_t defined in (A.8).

We are interested in the explicit dependence on the angles ϕ_h and ϕ_k. So it is useful to take some scalar products with p_h in the form

$$\begin{aligned}\frac{1}{2}V_{1,2}&=k_{1,2}p_h=a^{1,2}+b\cos\phi_h,\\\frac{1}{2}\mu R&=kp_h=R(a^k+b^k(\cos\phi_h\cos\phi_k+\sin\phi_h\sin\phi_k)).\end{aligned} \tag{9}$$

Also, we will use $a^\pm=a^2\pm a^1$. The explicit expressions for the coefficients are given in the Appendix, see (A.7).

3 The hadronic tensor and the Born approximation

The cross section of the electroproduction process can be obtained in terms of the convolution of leptonic and hadronic tensors. There are two leptonic tensors: with and without additional radiated photon. The Born leptonic tensor (without a photon) is standard, and the radiative one is cumbersome. The explicit expressions for the leptonic tensors and formulae for the RC in terms of them can be found in [14,15].

The hadronic tensor without the T- and P-odd terms can be presented in the form [16,17]

$$W^{\mu\nu}=-\tilde{g}^{\mu\nu}\mathcal{H}_1+\tilde{p}^\mu\tilde{p}^\nu\mathcal{H}_2+\tilde{p}_h^\mu\tilde{p}_h^\nu\mathcal{H}_3+(\tilde{p}^\mu\tilde{p}_h^\nu+\tilde{p}_h^\mu\tilde{p}^\nu)\mathcal{H}_4, \tag{10}$$

where

$$\tilde{g}^{\mu\nu}=g^{\mu\nu}+\frac{q^\mu q^\nu}{Q^2},\quad \tilde{p}^\mu=p^\mu+\frac{q^\mu pq}{Q^2},\quad \tilde{p}_h^\mu=p_h^\mu+\frac{q^\mu p_hq}{Q^2}, \tag{11}$$

and all of the SF depends on four kinematical invariants (for example, Q^2, W^2, t, z) The model for the structure functions can be constructed on the basis of results of the paper by Mulders and Tangerman [8]. Keeping only the leading twist contribution we have for the structure functions

$$\begin{aligned}\mathcal{H}_1&=\sum_q e_q^2f_q(x)D_q\mathcal{G},\\\mathcal{H}_2&=-\frac{p_\mathrm{t}^2+m_h^2}{M^2E_h^2}\sum_q e_q^2f_q(x)D_q\mathcal{G},\\\mathcal{H}_3&=0,\\\mathcal{H}_4&=\frac{1}{ME_h}\sum_q e_q^2f_q(x)D_q\mathcal{G},\end{aligned} \tag{12}$$

and

$$\mathcal{G}=\mathcal{G}_1=b_s\exp(-b_sp_\mathrm{t}^2), \tag{13}$$

where $b_s=R_b^2/z^2$ is a slope parameter and R_b is a parameter of the model. e_q, $f_q(x)$ and D_q are the charge, distribution and fragmentation function of the quark with flavour q. The expressions for the hadron energy E_h in the lab frame and its transversal momentum p_t are given in the Appendix; see (A.8).

The Born cross section has the following dependence on ϕ_h:

$$\sigma_0=\frac{\mathrm{d}\sigma_0}{\mathrm{d}x\mathrm{d}y\mathrm{d}z\mathrm{d}p_\mathrm{t}^2\mathrm{d}\phi_h}=\frac{N}{Q^4}(A+\cos\phi_hA^c+\cos2\phi_hA^{cc}), \tag{14}$$

where $N=\alpha^2yS_x/\lambda_Q^{1/2}$. The coefficients A do not depend on ϕ_h anymore and they have the form

$$\begin{aligned}A&=2Q^2\mathcal{H}_1+(SX-M^2Q^2)\mathcal{H}_2\\&\quad+(4a^1a^2+2b^2-M_h^2Q^2)\mathcal{H}_3\\&\quad+(2Xa^1+2Sa^2-zS_xQ^2)\mathcal{H}_4,\\A^c&=2b(2a^+\mathcal{H}_3+S_p\mathcal{H}_4),\\A^{cc}&=2b^2\mathcal{H}_3.\end{aligned} \tag{15}$$

When integrated over the kinematical variables ϕ_h and p_t the cross section (14) coincides with the well-known formula for the semi-inclusive cross section calculated within QPM

$$\sigma_{xyz} = \frac{\mathrm{d}\sigma}{\mathrm{d}x\mathrm{d}y\mathrm{d}z} = \frac{2\pi\alpha^2}{yQ^2}(y^2+2-2y)\sum_q e_q^2 f_q(x) D_q. \quad (16)$$

Unfortunately, the p_t^2 distribution

$$\frac{1}{\sigma_{xyz}}\frac{\mathrm{d}\sigma_{xyz}}{\mathrm{d}p_\mathrm{t}^2} \approx \mathcal{G}, \quad (17)$$

calculated with the exponential slope (13) does not fit the experimental data with sufficient χ^2. So the more complicated model [18] with a power dependence on p_t^2 seems to be more adequate. Another possibility to reach an agreement with the data consists in the replacement of the Gaussian factor (13) by the fit of the experimental p_t^2 distribution taken in the form [6]

$$\mathcal{G} = \mathcal{G}_2 = \left[\frac{1}{c_1 + c_2 z + p_\mathrm{t}^2}\right]^{c_3+c_4 z}. \quad (18)$$

4 The radiative correction of the lowest order

The cross section that takes into account radiative effects can be written as

$$\sigma_\mathrm{obs} = \sigma_0 \mathrm{e}^{\delta_\mathrm{inf}}(1+\delta_{VR}+\delta_\mathrm{vac}) + \sigma_F. \quad (19)$$

Here the corrections δ_inf and δ_vac come from radiation of soft photons [12] and the effects of vacuum polarization[1]. The correction δ_{VR} is an infrared-free sum of factorized parts of real and virtual photon radiation. These quantities are given by the following expressions:

$$\begin{aligned}
\delta_{VR} &= \frac{\alpha}{\pi}\left(\frac{3}{2}l_m - 2 - \frac{1}{2}\ln^2\frac{X'}{S'} + \mathrm{Li}_2\frac{S'X'-Q^2p_x^2}{S'X'} - \frac{\pi^2}{6}\right),\\
\delta_\mathrm{inf} &= \frac{\alpha}{\pi}(l_m-1)\ln\frac{(p_x^2-(M+m_\pi)^2)^2}{S'X'}, \quad (20)\\
\delta_\mathrm{vac} &= \delta_\mathrm{vac}^\mathrm{lept} + \delta_\mathrm{vac}^\mathrm{hadr},
\end{aligned}$$

where $S' = X+Q^2-V_2$, $X' = S-Q^2-V_1$, $l_m = \ln Q^2/m^2$ and Li_2 is the Spence function or dilogarithm.

The contribution of the radiative tail has the standard form [19,15]

$$\begin{aligned}
\sigma_F = -\frac{\alpha N}{2\pi}\int_0^{2\pi}\mathrm{d}\phi_k \int_{\tau_\mathrm{min}}^{\tau_\mathrm{max}}\mathrm{d}\tau \sum_{i=1}^{4}\sum_{j=1}^{3}\theta_{ij}(\tau,\phi_k)\times\\
\times\int_0^{R_\mathrm{max}}\mathrm{d}R R^{j-2}\left[\frac{\tilde{\mathcal{H}}_i}{(Q^2+R\tau)^2} - \delta_j\frac{\mathcal{H}_i}{Q^4}\right]. \quad (21)
\end{aligned}$$

Here $2M^2\tau_\mathrm{max,min} = S_x \pm \lambda_Q^{1/2}$ and $R_\mathrm{max} = (M_x^2-(M+m_\pi)^2)/(1+\tau-\mu)$, δ_j=1 for j=1 and δ_j=0 otherwise. The explicit formulae for the functions $\theta(\tau,\phi_k)$ can be found in the Appendix. The structure functions $\mathcal{H}_i$ are exactly the same as used for the Born cross section (see (12) for the model exploited in our paper), whereas $\tilde{\mathcal{H}}_i$ should be obtained from the $\mathcal{H}_i$ by replacing $q \to q-k$ in all kinematical variables (see (7), for example).

[1] There are explicit formulae for the leptonic contribution to the vacuum polarization effect (see [19] for example) and parameterization of hadronic one [20]

5 Numerical analysis

In this section we give numerical results for the RC to the semi-inclusive unpolarized cross section. For all cases the RC factor is defined as the ratio of observed to Born cross sections. Also we will speak about the relative RC (or simply RC), which is the difference between observed and Born cross sections or asymmetries divided by the Born ones.

For definiteness we choose the kinematics of the HERMES experiment at DESY. First, HERMES is a modern current experiment with rich possibilities for studies in semi-inclusive physics (see [7]). Second, HERMES is an experiment with an electron beam, so relatively large RCs with respect to the muon DIS experiment are anticipated.

The dependence of the RC on x, y and z is widely discussed in [4], where the quark-parton model is assumed. Similar results can be obtained using the formulae of this paper after integration over p_t and θ_h. In this paper we concentrate on a comparison of the codes constructed on the basis of the two sets of formulae and on studying of the effects beyond the quark-parton model: azimuthal asymmetries and dependencies on the transversal momentum p_t.

5.1 FORTRAN codes POLRAD 2.0 and HAPRAD

The special FORTRAN code HAPRAD was developed to calculate the RC to five-dimensional cross section, $\mathrm{d}^5\sigma/\mathrm{d}x\mathrm{d}y\mathrm{d}z\mathrm{d}p_\mathrm{t}^2\mathrm{d}\theta_h$. On the other hand there is the code POLRAD 2.0 with the special patch SIRAD, which calculated the RC to the semi-inclusive three-dimensional cross section obtained in QPM.

In this section we show that the numerical results for the RC to $\mathrm{d}\sigma/\mathrm{d}x\mathrm{d}y\mathrm{d}z$ reproduced by these two codes coincide with a good accuracy. This can be seen from Table 1. In this table we represent the RC to the cross section as it follows from runs of the codes POLRAD 2.0 and HAPRAD. Since HAPRAD allows one to take into account the kinematical cuts and to use different models for the p_t^2-slope, three fits for the p_t^2-distribution and the cases with and without experimental cuts were considered. The first fit for the p_t^2-slope is defined in (13), while the second and third ones are our fits of the experimental data [6] using exponential ($\mathcal{G}_1' = \mathcal{G}_1$ at $b_s = R_b^2/z$) and power (see (18)) functional forms. As the kinematical cuts on ϕ_h and p_t of the measured hadron we took the HERMES geometrical ones [22]. We can conclude from this analysis that neither important differences between the SIRAD and HAPRAD results, if an exponential model for the p_t^2-distribution is used, nor a dependence on the slope parameter model and applying of geometrical cuts are found. However, the RC takes a negative shift in the case of the model based on the power functional form (18). As is discussed below the RC depends on the steepness of the p_t^2-distribution. This is a reason why models like $\delta(p_\mathrm{t}^2)$ (QPM, POLRAD 2.0) and (13) give a larger RC. Within a practical RC procedure in a concrete measurement of

Table 1. The results for the RC factors of the three-dimensional semi-inclusive cross section obtained using the FORTRAN codes SIRAD and HAPRAD (see text for further explanation). The kinematical points are taken from Table 1 of [7]. The following parameters of the models of $G_{1,2}$ were used: c_1=0.642, c_2=0.637, c_3=4.91, c_4=-0.813, R_b^2=2 GeV^{-2}. The parton distributions were taken from [21]

x	y	Q^2	z	SIRAD	HAPRAD					
					without cuts			with cuts		
		GeV^2			$\mathcal{G}_1$	$\mathcal{G}_1'$	$\mathcal{G}_2$	$\mathcal{G}_1$	$\mathcal{G}_1'$	$\mathcal{G}_2$
0.038	0.677	1.33	0.25	1.029	1.033	1.024	0.982	1.041	1.025	0.985
0.062	0.567	1.82	0.35	0.996	0.989	0.989	0.947	0.989	0.980	0.951
0.092	0.529	2.52	0.45	0.970	0.961	0.961	0.934	0.961	0.956	0.936
0.131	0.499	3.38	0.55	0.945	0.936	0.933	0.912	0.934	0.931	0.906
0.198	0.476	4.88	0.65	0.918	0.902	0.902	0.889	0.897	0.897	0.881

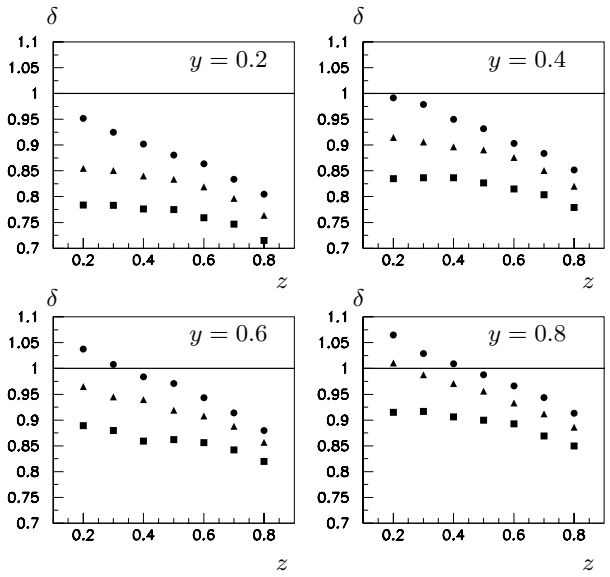

Fig. 1. Radiative correction to the semi-inclusive cross section for the kinematics of HERMES; $S^{1/2} = 7.19$ GeV. Symbols from top to bottom correspond to $x = 0.05$, 0.45 and 0.7. The results for $x = 0.15$ are skipped, because they practically coincide with the ones for $x = 0.05$

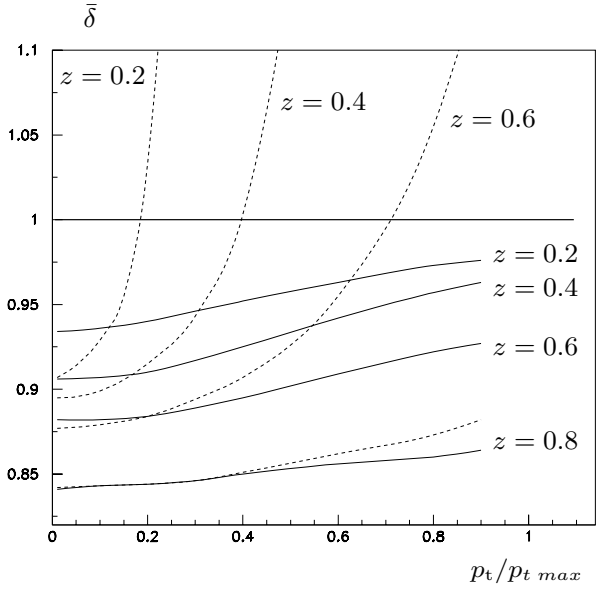

Fig. 2. Radiative correction to the semi-inclusive cross section vs. p_t; $(S)^{1/2} = 7.19$ GeV, $x = 0.15$, $Q^2 = 4$ GeV^2. Dashed and solid curves correspond to the models (13) and (18), respectively

$\mathrm{d}\sigma/\mathrm{d}x\mathrm{d}y\mathrm{d}z$ the model can be fixed only if the information on the p_t^2-distribution is considered additionally.

Also two models for the fragmentation function were considered: a simple parameterization of the pion data [23] and a modern model in the next-to-leading order QCD [24]. The RC factors calculated using these models differ by several percent. However, this model dependence is less important because it can be eliminated by applying an iteration procedure, where a fit of the extracted data is used for the RC calculation in a subsequent step.

5.2 Cross section and $\langle p_t^2 \rangle$

Here we give numerical results for unpolarized cross section in kinematics of experiment HERMES [22]. The RC factor (δ) to the semi-inclusive cross section integrated over p_t and ϕ_h as a function of x, y and z is presented in Fig. 1. Furthermore, we analyze the z and p_t dependence of the cross section and azimuthal asymmetries. The dependencies of the RC factor ($\bar{\delta} = \bar{\sigma}_{\mathrm{obs}}/\bar{\sigma}_{\mathrm{Born}}$) to the semi-inclusive cross section on the hadronic variables z and p_t are shown in Fig. 2, where sigma bar ($\bar{\sigma}$) is meant to denote the four-dimensional cross section $\mathrm{d}\sigma/\mathrm{d}x\mathrm{d}y\mathrm{d}z\mathrm{d}p_t^2$. We note that the obtained large correction to the cross section vs. p_t is an analog of the similar results for vector meson electroproduction [15]. In our case, the slope parameter depends on z (see (13)), so we have an important z-dependence of the effect. However, if the experimental fit for $\mathcal{G}$ is used (solid curves in the Fig. 2) there is no such rise of the RC for high p_t^2 values.

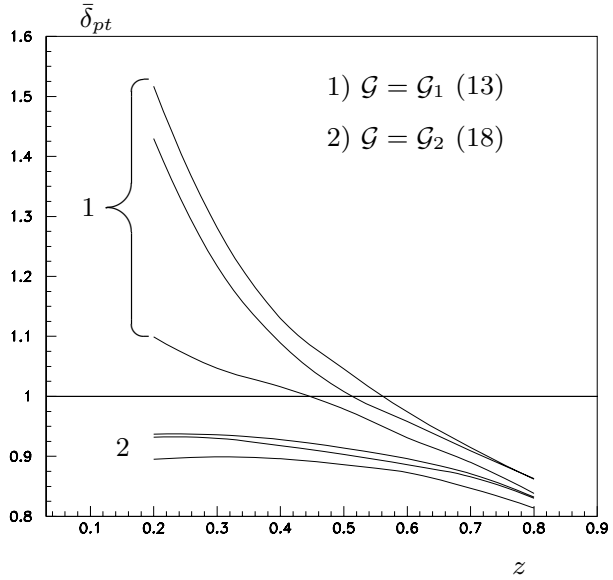

Fig. 3. Radiative correction to $\langle p_{\rm t}^2 \rangle$ defined in (24) for the HERMES kinematics, $(S)^{1/2} = 7.19\,\mathrm{GeV}$, $y = 0.4$. The curves from top to bottom correspond to $x = 0.15$, 0.05 and 0.45

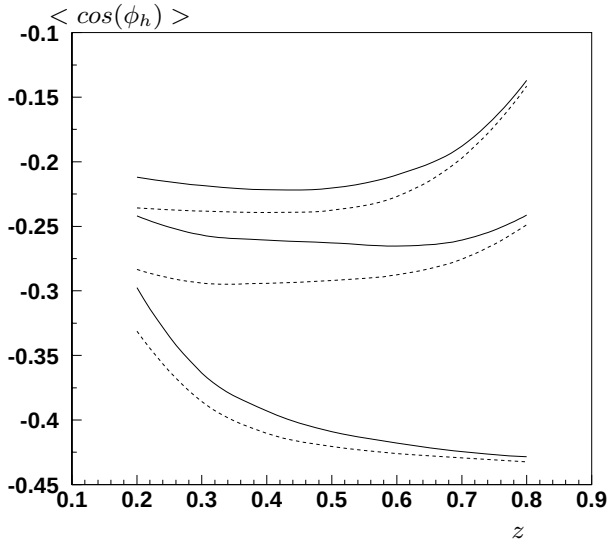

Fig. 4. Azimuthal asymmetry $\langle \cos\phi_h \rangle$ vs. z for $y = 0.2$ within the HERMES kinematics; $(S)^{1/2} = 7.19\,\mathrm{GeV}$. Dashed (solid) lines correspond to the Born (observed) asymmetries. Curves from top to bottom correspond to $x = 0.7$, 0.45 and 0.05

The quantity crucial for QCD predictions [1] $\langle p_{\rm t}^2 \rangle$ is expressed in terms of $\bar{\sigma}$ as

$$\langle p_{\rm t}^2 \rangle = \frac{\int \mathrm{d}p_{\rm t}^2 p_{\rm t}^2 \bar{\sigma}}{\int \mathrm{d}p_{\rm t}^2 \bar{\sigma}}. \tag{22}$$

The RC to this quantity can be expressed as

$$\delta_{pt} = \frac{\int \mathrm{d}p_{\rm t}^2 p_{\rm t}^2 \bar{\sigma}_{\rm obs}}{\int \mathrm{d}p_{\rm t}^2 \bar{\sigma}_{\rm obs}} \Big/ \frac{\int \mathrm{d}p_{\rm t}^2 p_{\rm t}^2 \bar{\sigma}_{\rm Born}}{\int \mathrm{d}p_{\rm t}^2 \bar{\sigma}_{\rm Born}} = \frac{\bar{\delta}_{pt}}{\delta}, \tag{23}$$

where

$$\bar{\delta}_{pt} = \frac{\int \mathrm{d}p_{\rm t}^2 p_{\rm t}^2 \bar{\sigma}_{\rm obs}}{\int \mathrm{d}p_{\rm t}^2 p_{\rm t}^2\ \bar{\sigma}_{\rm Born}},$$
$$\delta = \frac{\int \mathrm{d}p_{\rm t}^2 \bar{\sigma}_{\rm Born}}{\int \mathrm{d}p_{\rm t}^2 \bar{\sigma}_{\rm obs}}. \tag{24}$$

The correction δ is the semi-inclusive RC factor discussed above (see Fig. 1). The correction $\bar{\delta}_{pt}$ both for the exponential and for the power model (13), (18) is presented in Fig. 3.

Similar to the case of the $p_{\rm t}^2$-distribution, the radiative effect is larger when the exponential model (13) is used. That is because of the contribution of a small $\tilde{p}_{\rm t}^2$ when we integrate over the phase space of the emitted photon (21). The steeper the slope of the $p_{\rm t}^2$-distribution, the larger this contribution to the RC.

5.3 Azimuthal asymmetries

The following azimuthal asymmetries are measurable in the experiments [25]

$$\langle \cos\phi_h \rangle = \bar{\sigma}_{\rm obs}^{-1} \int_0^{2\pi} \mathrm{d}\phi_h \cos\phi_h \sigma_{\rm obs},$$

$$\langle \cos 2\phi_h \rangle = \bar{\sigma}_{\rm obs}^{-1} \int_0^{2\pi} \mathrm{d}\phi_h \cos 2\phi_h \sigma_{\rm obs},$$

$$\langle \sin\phi_h \rangle = \bar{\sigma}_{\rm obs}^{-1} \int_0^{2\pi} \mathrm{d}\phi_h \sin\phi_h \sigma_{\rm obs}. \tag{25}$$

In terms of these quantities the observed cross section (19) can be written as

$$\sigma_{\rm obs} = \bar{\sigma}_{\rm obs}\big(1 + \langle\cos\phi_h\rangle \cos\phi_h + \langle\cos 2\phi_h\rangle \cos 2\phi_h\big) + \sigma_{\rm add}. \tag{26}$$

Here $\sigma_{\rm add}$ originates from the contribution of the higher harmonics ($\sin\phi_h, \sin 2\phi_h, \cdots$). There are no contributions at the Born level (see (14)), and $\sigma_{\rm add}^{\rm Born} = 0$.

The azimuthal asymmetry $\langle \cos\phi_h \rangle$ is negative in the region considered. The RC to the quantity can exceed 10% The result is shown in Fig.4.

Within the model of (12) $\langle \cos 2\phi_h \rangle$ is equal to zero at the Born level. So the asymmetry in this case is defined by the RC only. Our estimation shows that this effect is of order 1%. The relative RC to the asymmetry can be estimated using another model [9], where $\langle \cos 2\phi_h \rangle \neq 0$ at the Born level. It is of order 10% in the region of applicability of the model.

$\langle \sin\phi_h \rangle$ is equal to zero at the Born level in any case. But there is a nonzero contribution to it coming from the RC. The numerical analysis shows that radiative corrections do not give a visible contribution to it. For the HERMES kinematical region, the values of $\langle \sin\phi_h \rangle$ do not exceed 10^{-4}.

We should stress that our predictions for the values of the radiative effects display a strong model dependence.

Therefore, any reliable method of radiative correction of the experimental data has to be based on an iterative procedure, where all necessary fits for the RC codes use the processing data as an input and are specified in every step of this procedure. This procedure can be readily developed on the basis of the code HAPRAD.

6 Discussion and conclusion

In this paper the QED radiative correction to different observable quantities in the experiments on hadron electroproduction is analyzed. The explicit covariant formulae are given in Sect. 4 and in the Appendix.

The new FORTRAN code HAPRAD is developed in order to perform the numerical analysis. It was shown in Sect. 5.1 that the results for the RC to the cross section integrated over $p_{\rm t}$ and ϕ_h are in agreement with POLRAD 2.0 [13]. Several models for the structure functions and slope parameter with respect to $p_{\rm t}^2$ were applied. It is found that the model based on a power $p_{\rm t}^2$-slope model leads to smaller values for the RC.

Within the exponential model for $\mathcal{G}$ (13) the RC to $\langle p_{\rm t}^2\rangle$ can exceed 40%. However, it essentially depends on the model of the $p_{\rm t}^2$-distribution as well as on x and z.

The RC to the azimuthal asymmetries is of order 10%. The asymmetry $\langle \sin\phi_h\rangle$ due to the RC is found to be negligible but not equal to zero exactly.

The FORTRAN code HAPRAD is available (aku@hep.by) for the calculation of the RC to observable quantities in the experiments on hadron electroproduction.

Acknowledgements. We are grateful to H. Avakian, A. Brull, H. Ihssen, R. Milner, K. Oganessyan and H. Spiesberger for fruitful discussions and comments.

Appendix

In this appendix we list the explicit form for the functions θ_{ij}:

$$\theta_{ij}(\tau,\phi_k)=\theta^0_{ij}+\cos\phi_h\theta^c_{ij}+\sin\phi_h\theta^s_{ij}+\cos 2\phi_h\theta^{cc}_{ij}, \quad \text{(A.1)}$$

where

$$\theta^0_{12}=4\tau F_{\rm IR},$$

$$\begin{aligned}\theta^0_{22}=&-\frac{1}{2}F_dS_p^2\tau+\frac{1}{2}F_{1+}S_pS_x\\&+F_{2-}S_p+2F_{2+}M^2\tau\\&-2F_{\rm IR}M^2\tau+F_{\rm IR}S_x,\end{aligned}$$

$$\begin{aligned}\theta^0_{32}=&2(-2F_db^2\tau-F_d(a^+)^2\tau-F_{1+}a^-a^+\\&+2F_{2-}\cos\phi_kbb^k+2F_{2-}a^ka^+\\&-F_{\rm IR}M_h^2\tau-2F_{\rm IR}a^ka^-),\end{aligned}$$

$$\begin{aligned}\theta^c_{32}=&4(-2F_dba^+\tau-F_{1+}ba^-+F_{2-}\cos\phi_kb^ka^+\\&+2F_{2-}ba^k-\cos\phi_kF_{\rm IR}b^ka^-),\end{aligned}$$

$$\theta^{cc}_{32}=4b(-F_db\tau+F_{2-}\cos\phi_kb^k),$$

$$\theta^s_{32}=4b^k\sin\phi_k(F_{2-}a^+-F_{\rm IR}a^-),$$

$$\begin{aligned}\theta^0_{42}=&-2F_da^+S_p\tau-F_{1+}a^-S_p+F_{1+}a^+S_x\\&+2F_{2-}a^kS_p+2F_{2-}a^++2F_{2+}\tau zS_x\\&+F_{\rm IR}a^kS_x-2F_{\rm IR}a^--2F_{\rm IR}\tau zS_x,\end{aligned}$$

$$\begin{aligned}\theta^c_{42}=&2(-2F_dbS_p\tau+F_{1+}bS_x+F_{2-}\cos\phi_kb^kS_p\\&+2F_{2-}b+\cos\phi_kF_{\rm IR}b^kS_x),\end{aligned}$$

$$\theta^s_{42}=2b^k\sin\phi_k(F_{2-}S_p+F_{\rm IR}S_x),$$

$$\theta^0_{13}=-2(F+F_d\tau^2),$$

$$\theta^0_{23}=2FM^2+F_dM^2\tau^2-\frac{1}{2}F_dS_x\tau-\frac{1}{2}F_{1+}S_p,$$

$$\begin{aligned}\theta^0_{33}=&2FM_h^2+F_dM_h^2\tau^2+2F_da^ka^-\tau\\&-2F_{1+}\cos\phi_kbb^k-2F_{1+}a^ka^+,\end{aligned}$$

$$\theta^c_{33}=2(F_d\cos\phi_kb^ka^-\tau-F_{1+}\cos\phi_kb^ka^+-2F_{1+}ba^k),$$

$$\theta^{cc}_{33}=-2F_{1+}\cos\phi_kbb^k,$$

$$\theta^s_{33}=2b^k\sin\phi_k(F_da^-\tau-F_{1+}a^+),$$

$$\begin{aligned}\theta^0_{43}=&2FzS_x-F_da^kS_x\tau+F_da^-\tau+F_d\tau^2zS_x\\&-F_{1+}a^kS_p-F_{1+}a^+,\end{aligned}$$

$$\theta^c_{43}=-F_d\cos\phi_kb^kS_x\tau-F_{1+}\cos\phi_kb^kS_p-2F_{1+}b,$$

$$\theta^s_{43}=-b^k\sin\phi_k(F_dS_x\tau+F_{1+}S_p). \quad \text{(A.2)}$$

Here

$$F_{1+}=\frac{F}{z_1}+\frac{F}{z_2},\ F_{2+}=F\left(\frac{m^2}{z_2^2}+\frac{m^2}{z_1^2}\right),$$

$$F_{2-}=F\left(\frac{m^2}{z_2^2}-\frac{m^2}{z_1^2}\right),\ F_d=\frac{F}{z_1z_2}, \quad \text{(A.3)}$$

where $F=1/(2\pi\sqrt{\lambda_Q})$ and

$$F_{\rm IR}=F_{2+}-Q^2F_d. \quad \text{(A.4)}$$

The quantities $z_{1,2}=kk_{1,2}/kp$ can be expressed in terms of integration variables as

$$\begin{aligned}z_1&=\lambda_Q^{-1}\big(Q^2S_p+\tau(SS_x+2M^2Q^2)-2M\cos\phi_k\sqrt{\lambda_\tau\lambda}\big),\\z_2&=\lambda_Q^{-1}\big(Q^2S_p+\tau(XS_x-2M^2Q^2)-2M\cos\phi_k\sqrt{\lambda_\tau\lambda}\big),\end{aligned} \quad \text{(A.5)}$$

where

$$\lambda_\tau = (\tau - \tau_{\min})(\tau_{\max} - \tau), \quad \lambda = SXQ^2 - M^2Q^4 - m^2\lambda_Q. \tag{A.6}$$

The scalar products of p_h (see (9)) are expressed via coefficients a^1, a^2, b, a^k and b^k:

$$\begin{aligned} 2Ma^1 &= SE_h - (SS_x + 2M^2Q^2)p_l\lambda_Q^{-1/2}, \\ 2Ma^2 &= XE_h - (XS_x - 2M^2Q^2)p_l\lambda_Q^{-1/2}, \\ b &= -p_{\rm t}\sqrt{\lambda/\lambda_Q}, \\ 2Ma^k &= E_h - p_l(S_x - 2M^2\tau)\lambda_Q^{-1/2}, \\ b^k &= -Mp_{\rm t}\sqrt{\lambda_\tau/\lambda_Q}. \end{aligned} \tag{A.7}$$

The quantities E_h, P_l and P_t are invariants

$$\begin{aligned} E_h &= z\nu = \frac{zS_x}{2M}, \\ \frac{p_l\sqrt{\lambda_Q}}{M} &= t - M_h^2 + Q^2 + 2\nu E_h, \\ p_{\rm t}^2 &= E_h^2 - p_l^2 - M_h^2. \end{aligned} \tag{A.8}$$

In the rest frame they make sense of the energy, the longitudinal and transversal momenta of the final hadron.

References

1. H. Georgi, H.D. Politzer, Phys. Rev. Lett. **40**, 3 (1978)
2. L.W. Mo and Y.S. Tsai, Rev. Mod. Phys.**41**, 205 (1969); Y.S. Tsai, SLAC-PUB-848 (1971)
3. D.Yu. Bardin, N.M. Shumeiko, Nucl. Phys. B **127**, 242 (1977)
4. A.V. Soroko, N.M. Shumeiko, Yad.Fiz. **49**, 1348 (1989)
5. A. Kwiatkowski, H. Spiesberger, H.J. Möhring, Comp. Phys. Comm. **69**, 155 (1992)
6. EMC Collab., J. Ashman et al., Z. Phys. C **52**, 361 (1991)
7. HERMES Collab. K. Ackerstaff et al., Phys. Rev. Lett. **58**, 5519 (1998)
8. P.J. Mulders, R.D. Tangerman, Nucl. Phys. B **461**, 197 (1996), Erratum ibid. B **484**, 538 (1996)
9. A. Brandenburg, V.V. Khoze, D. Muller, Phys. Lett. B **347**, 413 (1995)
10. K.A. Oganessyan, H.R. Avakian, N. Bianchi, P. Di Nezza, Eur. Phys. J. C **5**, 681 (1998)
11. D.R. Yennie, S. Frautchi, H. Suura, Ann. Phys. (N.Y.) **13**, 379 (1961)
12. N.M. Shumeiko, Sov. J. Nucl. Phys. **29**, 807 (1979)
13. I. Akushevich, A. Ilyichev, N. Shumeiko, A. Soroko, A. Tolkachev, Comp. Phys. Comm. **104**, 201 (1997)
14. I.V. Akushevich, A.N. Ilyichev, N.M. Shumeiko, J. Phys. G **24**, 1995 (1998)
15. I. Akushevich, Eur. Phys. J. C **8**, 457 (1999)
16. K. Hagiwara, K. Hikasa, N. Kai Phys. Rev. D **27**, 84 (1983)
17. N.K. Pak, Ann. Phys. **104**, 54 (1977)
18. R. Jakob, P.J. Mulders, J. Rodrigues, Nucl. Phys. A **626**, 937 (1997)
19. I.V. Akushevich, N.M. Shumeiko, J. Phys. G**20**, 513 (1994)
20. H. Burkhardt, B. Pietrzyk, Phys. Lett. B **356**, 398 (1995)
21. M. Glueck, E. Reya, A. Vogt, Z. Phys. C **53**, 127 (1992)
22. HERMES, Technical design report, 1993
23. EMC Collab., J.J. Aubert et al., Phys. Lett. B **160**, 417 (1985)
24. J. Binnewies, B.A. Kniehl, G. Kramer, Z. Phys. C **65**, 471 (1995)
25. EMC Collab., M. Arneodo et al, Z. Phys. C **34**, 277 (1987)